Published by
NIGERIAN SOCIETY OF PHYSICAL SCIENCES
Available online @ https://journal.nsps.org.ng/index.php/jnsps

J. Nig. Soc. Phys. Sci. 7 (2025) 2938

Journal of the Nigerian Society of Physical Sciences

Deep neural network model for vertical total electron content prediction at a single low latitude station

F. U. Salifu[a,b,*], O. A. Oladipo[a], E. O. Ebock[a], B. Nava[c]

[a]*Physics Department, University of Ilorin, Ilorin, Nigeria*
[b]*Department of Physics, Confluence University of Science and Technology, Osara, Nigeria*
[c]*The Abdus Salam International Centre for Theoretical Physics (ICTP), Trieste, Italy*

Abstract

Modeling ionospheric parameters at low and equatorial stations is quite challenging due to the nature of the variation in the region. In this study, a Deep Neural Network (DNN) was configured via optimization of its hyperparameters and then trained to predict vertical Total Electron Content (vTEC) at a single low latitude location. Input parameters to the model are universal time, day of the year and solar activity index (EUV / $F_{10.7}$), while the target parameter is vTEC at a single location. EUV and $F_{10.7}$ values were used separately as the solar ionizing index leading to two trained models. The data used for training were for the solar cycle 24 and the data were split into 75 % for training and 25 % for validation. The training process was completed by the number of iterations. In addition, the derived model was also validated using data for the whole of 2000 and 2021 which are years outside the solar cycle 24. For completeness, the two models were also compared with NeQuick 2 model which is a global empirical model. The results obtained showed that the DNN models were able to predict reasonably well within the solar cycle 24 and slightly outperformed NeQuick 2 model. Similar results were obtained when the models were validated in 2021 with DNN performing slightly better than NeQuick 2 model. However, large deviation was recorded in 2000 – the DNN and NeQuick 2 models underestimated vTEC.

DOI:10.46481/jnsps.2025.2938

Keywords: Deep learning neural network, TEC model, Solar activity proxy, NeQuick 2

Article History :
Received: 16 May 2025
Received in revised form: 17 July 2025
Accepted for publication: 14 August 2025
Available online: 25 August 2025

Communicated by: I. B. Okon

1. Introduction

The ionosphere is the ionized region of the upper atmosphere. The region is being used for HF communication links and it is also an important factor to consider in Global Navigation Satellite System (GNSS) positioning and navigation. The formation of the ionosphere is due to photoionization of the neutral species in the upper atmosphere by the extreme ultraviolet (EUV) component of the solar radiation spectrum. There are different parameters being used to quantify the level of ionization in the ionosphere e.g. electron density profile (N(h)), peak parameters of each of the layers and Total Electron Content (TEC) among others. Models' prediction of these parameters is important for effective use of the ionosphere for HF communication links and GNSS signals for positioning and navigation. To this end, there exist several ionosphere models for the prediction of various parameters of the ionosphere - notable among the models are the International Reference Ionosphere (IRI) and the NeQuick [1–3]. IRI and NeQuick models are widely used global models and the two are semi-empirical models. This implies that the models are based on theoretical principles and empirical or experimental data. The performance of such models is based on availability of quality data across the globe. Assessment studies of the performance of the two models have been

*Corresponding author Tel. No.: +234-706-872-2371.
Email address: salifufu@custech.edu.ng (F. U. Salifu)

investigated and the results showed overestimation or underestimation at different geographic latitudes [4–10].

In recent time, Artificial Neural Network (ANN) or simply Neural Network (NN) has become a good tool for modeling different ionospheric parameters [11–17]. NN models are very effective in modelling complex and non-linear systems, and they give better performance over empirical/semi-empirical models [11, 12]. This is because NN models can learn complex variation in data and adjust the model's parameters accordingly to give better predictions unlike the empirical/semi-empirical models. DNN models are well-known to outperform ordinary NN because it can learn complex and non-linear systems more effectively [17]. For example, Ref. [11] developed a near real-time global foF2 empirical model using Neural Network technique. In training the model, the target parameter were the hourly daily values of foF2 from 26 worldwide ionospheric stations from 1976 to 1986, while the input parameters were the geophysical parameters of the training stations in addition to time, day of the year and solar activity proxy. In order to predict foF2 in real-time, recent observation of foF2 from 4 stations selected as control stations were also used as input. Results obtained showed temporal and spatial correlation between the model predictions and the observed values even during geomagnetic storms.

The studies cited above were based on predefined network models like, convolutional neural network (CNN), long short-term memory (LSTM) neural network, Attention Mechanism Neural Network, back-propagation artificial neural network (BPANN), EXtreme Gradient Boosting over Decision Trees (XGBoost or XGBDT) [14–17]. Also, a Hybrid Network which involves combination of two models has been used (e.g. CNN-LSTM-Attention Mechanism Neural Network [15]). The hybrid network makes use of weak models to build a single model that takes advantages of each of the weak models. Studies on Deep learning NN to model ionospheric parameters are rare. Deep artificial neural networks often provide high precision modeling when the number of training samples are large, but the challenge is to find optimal parameters that define the network architecture [17].

Modelling ionospheric parameter in the low latitude is quite challenging because of the nature of the variation in the region. The aim of the study is to train Deep NN (DNN) for Ilorin, a low latitude station, and to assess the performance of the model.

2. Configuration of the deep learning model and the data used

In this study, DNN was configured and trained unlike the studies cited in Section 1 where NN or hybrid neural network were used. It is well known that a DNN configuration consists of the input layer, the hidden layers with each having a specific number of neurons and the output layer. The input layer in the current study has three parameters i.e. Universal Time (UT), day of the year (DOY) and EUV or the solar radio flux at 10.7 cm ($F_{10.7}$), while the output layer has a single parameter i.e. vTEC at a single location. The number of hidden layers and the number of neurons/nodes per hidden layer were selected via an optimization process – i.e. the number of hidden layers with the number of neurons that minimizes the mean absolute error at the validation stage. It is important to mention that in selecting the right configuration (i.e. the number of hidden layers and neuron numbers), a fixed batch number and epoch number of 16 and 50 were used respectively for the training. Nine (9) configurations were considered (i.e. configurations with 1 hidden layer up to 9 hidden layers) and for each of the 9 configurations, training and validation were done and the mean absolute error (*mae*) was obtained. The configurations are such that the number of neurons increases with increase in the number of hidden layers. The well-known concepts of starting with high number of neurons for the first hidden layer and gradually reducing it was employed. The configuration with the minimum *mae* was selected as the optimal configuration.

The batch number and the epoch number at the training stage were also selected via an optimization process - as done for the number of hidden layers / neurons number. The batch number was varied in power of 2 from 8 to 64 (i.e. from 2^3 to 2^6) and the epoch number was varied from 50 in step of 50 up to 500. The batch and epoch number that minimize the *mae* for the optimal configuration were selected and these were used in this study.

In compiling the model for both the preliminary processes of optimization and the actual training of the optimal configuration, adamax was used as optimizer, mean square error as loss and mean absolute error as the performance metric. Fully connected layers were ensured by using Rectified Linear Unit (ReLU) that ensures back propagation as the activation function for both the hidden layers and the output layer. It is important to mention that the input parameters were normalized – this was to prevent the sensitivity of DNN to the magnitude and the range of values of each of the input parameters. Similarly, the data were split into 75 % for training and 25 % for validation. The training process was completed by the number of iterations.

The data used for this study were obtained from CODE's (Center for Orbit Determination in Europe) Global Ionospheric Map [18] for the increasing face of solar cycle 24 i.e. from 2009 to 2014. The two models developed based on $F_{10.7}$ as solar ionizing index and EUV as solar ionizing index were also validated using data for the whole years 2000 and 2021 i.e. data outside of solar cycle 24. The performance of the derived DNN models were compared with that of the NeQuick 2 [7] run in standard mode.

Deviation of the models' predictions from the observation was analyzed using correlation coefficient (r), coefficient of determination (r^2), root mean square error (*rmse*) and Index of Agreement ($IofA$). Index of agreement [19] is as defined in equation (1):

$$IofA = 1 - \frac{\sum_{i=1}^{n} (O_i - P_i)^2}{\sum_{i=1}^{n} \left(\left|P_i - \overline{O}\right| + \left|O_i - \overline{O}\right|\right)^2}, \tag{1}$$

where O is the observed, P is the predicted and $\overline{O}$ is the average observed values. The value of $IofA$ ranges from 0 to 1, where 0 means no agreement and 1 indicates a perfect agreement. Unlike correlation coefficient which indicates linearity

between two sets of values, $Io fA$ in addition indicates the closeness of the two sets of values.

3. Results obtained and discussions

Table 1 shows *mae* values against the number of hidden layers /neurons number for the optimization process of the DNN model configuration. The purpose of the process was to determine the appropriate number of hidden layers in the DNN model that is suitable for the dataset. As clearly seen in the table, the highest *mae* value of 7.14 TECu (TECu is TEC unit and $1\ TECu = 10^{16}$ electrons per square meter) was recorded for the configuration with 1 hidden layer and 8 neurons in the only hidden layer. The value decreases with increase in the number of hidden layers up to a configuration with 4 hidden layers with *mae* of 3.06 TECu. Raising or increasing the number of hidden layers further after 4 does not bring any substantial reduction in *mae* value. It is important to mention that the value of *mae* for the configuration with 7 hidden layers is due to wrong initialization of the model during training. A configuration with 4 hidden layers with the number of neurons in each layer as indicated in Table 1 was selected for this study as the optimal configuration.

The optimal configuration (i.e. configuration with 4 hidden layers) was further optimized by varying the epoch number and batch number during training. The value of *mae* for different combinations of epoch number and batch number at validation stage is indicated in Table 2. Except for the erroneous value of 27.30 TECu recorded in four instances, there is no significant variation in the values. Largely, the values of *mae* range between 3.15 and 2.84 TECu. Both epoch and batch numbers determine the length of training – if not appropriately selected it could lead to underfitting or overfitting. Epoch number is known to be the number of passes through the whole training dataset while batch number or batch size is the number training samples to work through before the model's internal parameters are updated. For the current study a combination of epoch number of 300 and batch size of 32 was selected – the *mae* value for this combination is 2.92 TECu.

Therefore, the DNN configuration shown in Figure 1 was used as the optimal configuration. The input layer has three parameters i.e. UT, DOY and $F_{10.7}$ or EUV – the parameters were pre-processed via normalization before feeding it as input into the first hidden layer. The essence of normalization is to scale the input parameters to a similar range e.g. 0 to 1 or -1 to 1. This is to prevent feature domination of parameters with large value in the learning process – thereby improving the accuracy of the trained model. The model has four hidden layers with neurons number of 32, 24, 16 and 8 for hidden layers 1, 2, 3 and 4 respectively. Rectified Linear Unit (ReLU) was used as the activation function for both the hidden layers and the output layer. The output layer is also dense and has a single output i.e. vTEC. In compiling the model, adamax was used as optimizer, mean square error as loss and mean absolute error as the performance metric. The layers are dense and fully connected.

The diurnal plot of the model values and the observed values is shown in column (i) of Figure 2. It is clearly seen how the

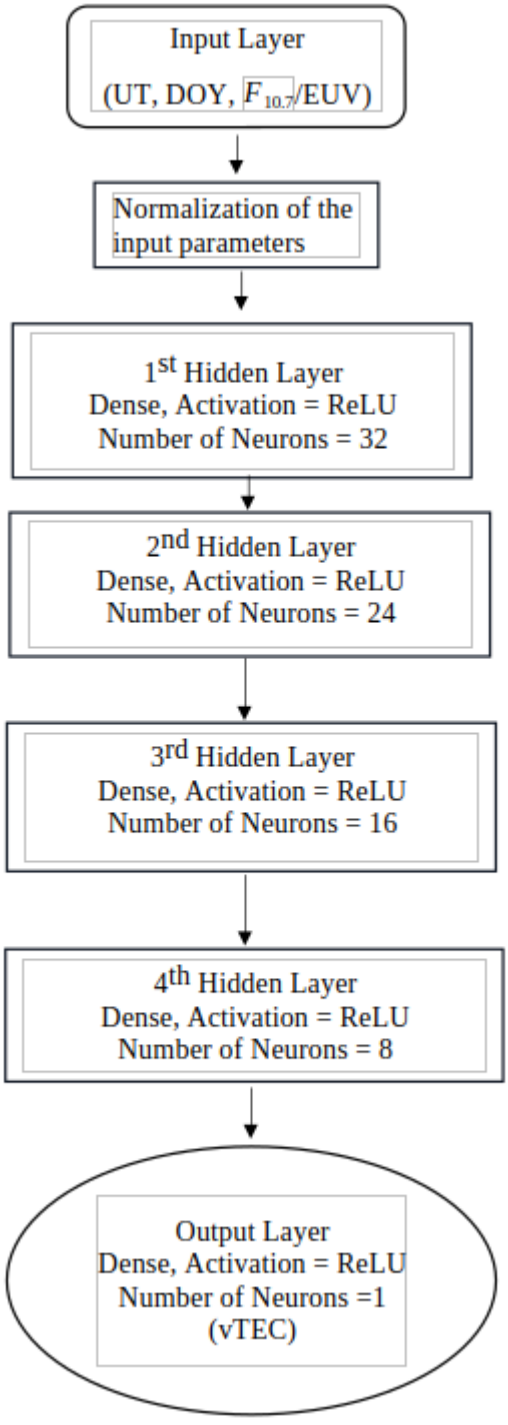

Figure 1: Schematic view of the optimal configuration. The training process was completed by the number of iterations.

predictions of each of the three models are close to the observed values – model driven with $F_{10.7}$ shows a better performance compared to the DNN driven by EUV and NeQuick 2 model. The *mae* value clearly indicates the performance of the three models in which *mae* of 2.88 TECu, 3.20 TECu and 6.92 TECu were recorded for DNN driven with $F_{10.7}$, DNN driven by EUV and NeQuick 2 model respectively. Error in the current study

Table 1: Performance of models in *mae* for different number of hidden layers / number of neurons is indicated in the table. The *mae* value for the configuration with 7 hidden layers is due to wrong initialization during training.

Total Number of Hidden Layers	Number of Neurons in Hidden Layer									*mae* in TECu
	1	2	3	4	5	6	7	8	9	
1	8									7.14
2	16	8								4.85
3	24	16	8							4.40
4	32	24	16	8						3.06
5	40	32	24	16	8					3.08
6	48	40	32	24	16	8				3.00
7	56	48	40	32	24	16	8			27.30
8	64	56	48	40	32	24	16	8		3.06
9	72	64	56	48	40	32	24	16	8	2.93

Table 2: Mean absolute error in TECu at validation stage as a function of epoch number and batch number for the optimal configuration. The *mae* of 27.30 TECu indicates erroneous value due to wrong initialization of the parameters of the model during training process.

Epoch No.	Batch Number					
	4	8	16	32	64	128
50	3.05	3.00	3.11	3.31	3.29	3.60
100	3.00	2.97	27.30	3.07	3.14	27.30
150	3.01	3.02	2.99	2.93	3.03	3.18
200	2.96	3.15	3.01	2.95	3.00	3.04
250	2.96	2.97	2.95	2.94	3.08	3.14
300	2.93	2.95	2.98	2.92	2.99	3.00
350	3.02	3.00	3.02	2.95	3.03	2.99
400	27.30	2.88	2.88	2.98	2.96	2.96
450	27.30	2.92	2.97	2.96	3.00	3.02
500	2.84	2.94	2.94	2.98	2.95	2.97

is defined as the observed vTEC minus the model values – the positive *mae* values is an indication of a net underestimation. Plots in column (ii) of Figure 2 show the correlation plot between the model and the observed values for the three models. The values of r, r^2, $IofA$ and $rmse$ are indicated on each plot. The performance of the two DNN models when $F_{10.7}$ (a) and EUV (b) were used as the solar activity indices as well as that of the NeQuick 2 (c) is clearly seen in the plots. The fit is good for all the models – although a better fit is seen in the two DNN Models compared to the NeQuick 2. In terms of the correlation, coefficient of determination, root mean square error and index of agreement, DNN model driven with $F_{10.7}$ performed slightly better than the DNN driven with EUV and the NeQuick 2. The results showed that $F_{10.7}$ as solar index gives better results (marginally) with $r = 0.98$, $r^2 = 0.95$, $IofA = 0.99$ and $rmse = 4.02\ TECu$. This is followed closely by DNN driven with EUV with $r = 0.97$, $r^2 = 0.94$, $IofA = 0.98$ and $rmse = 4.46\ TECu$ and the values for the NeQuick 2 are $r = 0.89$, $r^2 = 0.80$, $IofA = 0.90$ and $rmse = 10.07\ TECu$. The results showed that models with $F_{10.7}$ and EUV as solar activity indices are of comparable performance and the two outperformed NeQuick 2 model.

Therefore, the DNN configuration shown in Figure 1 was used as the optimal configuration. The model has four hidden layers with neurons number of 32, 24, 16 and 8 for hidden layers 1, 2, 3 and 4 respectively. ReLU was used as the activation function for both the hidden layers and the output layer. In compiling the model, adamax was used as optimizer, mean square error as loss and mean absolute error as the performance metric. The layers are dense and fully connected.

Column (i) of Figure 3 shows the plots of modeled vs. observed vTEC for the three models i.e. (a) DNN driven with $F_{10.7}$, (b) DNN driven with EUV and NeQuick 2 for 2021 validation. Year 2021 is a low solar activity year and it is outside of the solar cycle 23 used for the training of the DNN model. It is clearly seen how each model predictions fit into the observed values – model driven with $F_{10.7}$ shows a better fitting. The fit is good for all the models – although a slightly better fit is seen in the two DNN Models compared to NeQuick 2 in terms of correlation coefficient, coefficient of determination. However, NeQuick 2 showed a better fit in terms of root mean square error and index of agreement. The results showed that $F_{10.7}$ as solar index gives better results (marginally) with $r = 0.93$, $r^2 = 0.87$, $IofA = 0.81$ and $rmse = 12.83\ TECu$. EUV statistics shows that $r = 0.93$, $r^2 = 0.86$, $IofA = 0.83$ and $rmse = 11.80\ TECu$ while NeQuick 2 model shows that $r = 0.91$, $r^2 = 0.83$, $IofA = 0.93$ and $rmse = 4.87\ TECu$. The values showed a better fit for DNN models in terms of correlation coefficient, coefficient of determination, while values of root mean square error and index of agreement showed that NeQuick 2 outperformed DNN models. Plots in column (ii) of Figure 3 show the distribution of errors for the three models – corresponding to that in column (i). Negative skewness is seen in the two DNN models – indicating overestimation of vTEC values while positive skewness is seen in NeQuick 2 model which indicates underestimation. The error ranges from -48.76 TECu to 6.50 TECu for the DNN driven with $F_{10.7}$, the value ranges from -45.00 TECu to 7.41 TECu and -11.96 TECu to 30.69 TECu respectively for DNN driven with EUV and NeQuick 2 model respectively. All these indices indicate that NeQuick 2 slightly outperformed DNN for year 2021 which is a year of low solar activities.

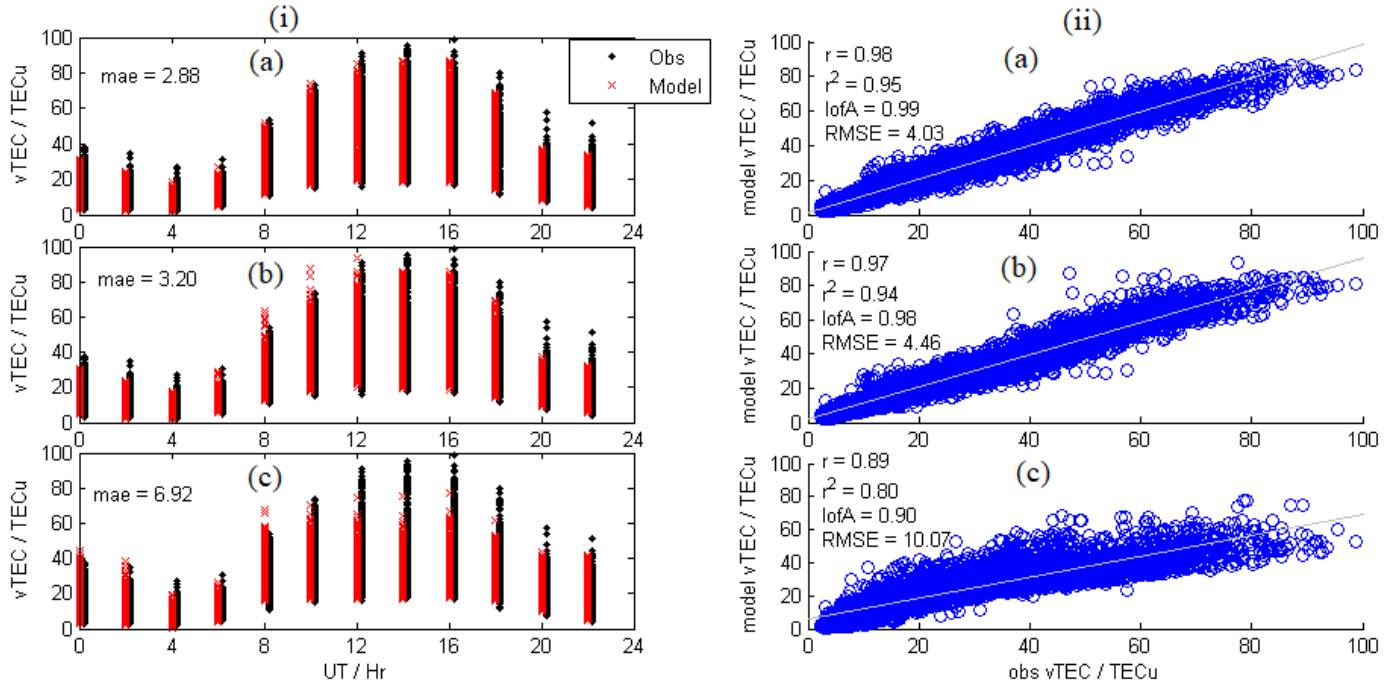

Figure 2: Corresponding diurnal plots of VTEC for the observed and models' predictions for the 25% validation data for (a) DNN model driven with $F_{10.7}$ (b) DNN model driven with EUV and (c) NeQuick 2 driven with daily $F_{10.7}$ values.

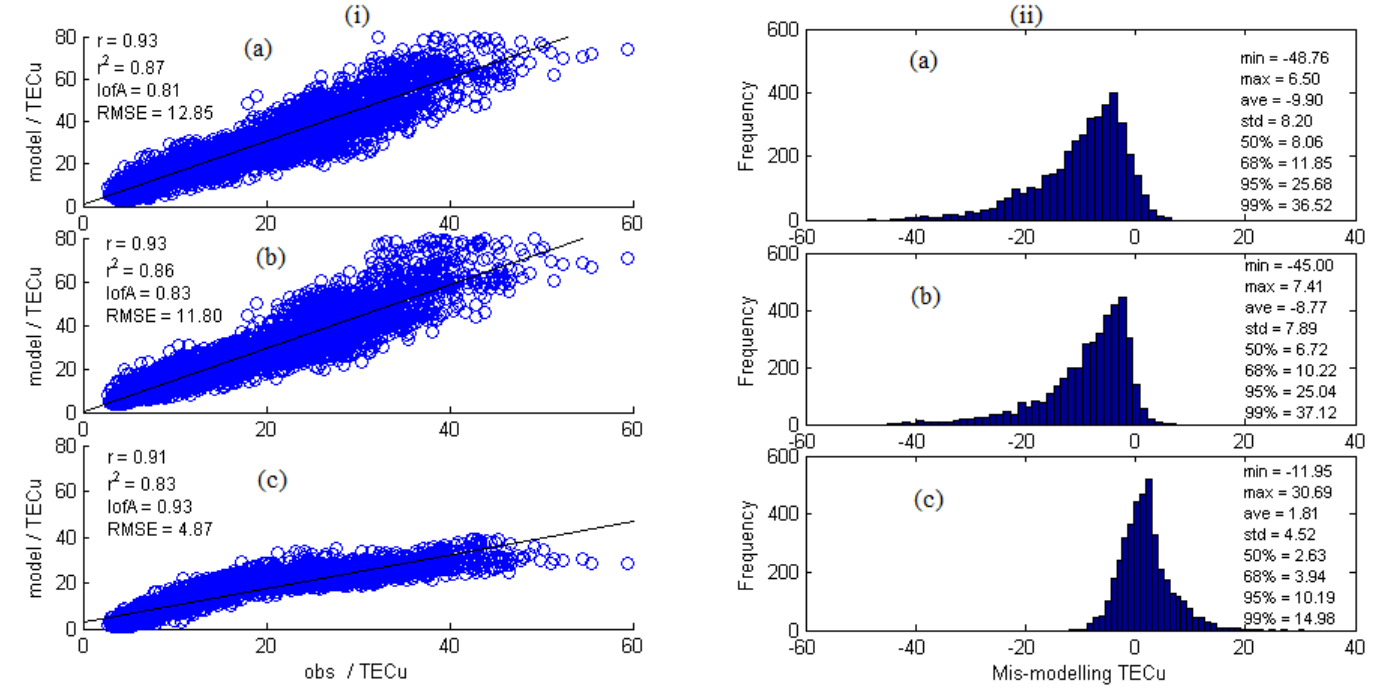

Figure 3: Diurnal plots of VTEC for the observed and models' predictions for 2021data for (a) DNN model driven with $F_{10.7}$ (b) DNN model driven with EUV and (c) NeQuick 2 driven with daily $F_{10.7}$ values. Column (ii) is for the corresponding error in which error is defined as the observed value minus the model value. Negative skewness is seen in DNN while positive skewness is seen in NeQuick 2 model.

The performance of the models was also tested in year 2000 by going back in time to see what the performance would look like during a solar maximum year with higher solar activity compared to that of solar cycle 24. It is important to mention that year 2000 is the solar maximum of solar cycle 23 and that data of higher solar activity like this were not used

in the training (indeed, maximum solar activity of solar cycle 24 was much lower than maximum solar activity of solar cycle 23). Year 2000 study was limited to the NeQuick 2 and DNN driven with $F_{10.7}$; this is because EUV data were not available for year 2000. Figure 4 shows the plots for 2000 which is a year of solar maximum outside of solar cycle 23 – same as Figure 3. It is clearly seen from column (i) of Figure 4 how the two models fit into the observed – the spread of data points around the fit line is an indication of the fitting. It is clearly seen that the spread is wider for DNN compared to NeQuick 2 model. The results showed that DNN is with $r = 0.85$, $r^2 = 0.72$, $IofA = 0.70$ and $rmse = 31.08\ TECu$, while NeQuick 2 model statistics shows that $r = 0.85$, $r^2 = 0.72$, $IofA = 0.72$ and $rmse = 22.8924\ TECu$. The values showed a better fit (marginally) for NeQuick 2 compared to DNN models driven with $F_{10.7}$. Plots in column (ii) of Figure 4 show the distribution of errors for the two models – corresponding to that in column (i). Positive skewness is seen in the two models i.e. DNN models driven with $F_{10.7}$ and NeQuick 2 model – indicating underestimation of vTEC values. The error ranges from -11.14 TECu to 78.51 TECu for the DNN driven with $F_{10.7}$and the value ranges from -30.63 TECu to 63.03 TECu for NeQuick 2 model. All these indices indicate that NeQuick 2 slightly outperformed DNN for year 2000 which is a year of solar maximum for solar cycle 22.

The result obtained in the current study is comparable to those of the recent studies on DNN models for the prediction of vTEC at low latitude stations in the African, American and Asian sectors [15, 20, 21, 23]. A study was done over Ethiopia in the African sector and machine learning (ML) algorithm based on the Support Vector Machine (SVM), LSTM Neural Network were used [20]. Data used for the study were GPS derived TEC from three stations at Addis Ababa, Urge, and Negele during the years 2013 to 2016. Their results were compared with IRI model unlike the current study in which NeQuick model was used as a standard model. The results obtained showed that SVM model predicted the hourly TEC variation with RMSE values between 2.136 TECu and 7.923 TECu, while RMSE values of between 1.483 and 2.527 TECU were obtained for LSTM model and RMSE values of between 4.777 and 14.519 TECU were obtained for IRI 2016 model. These results are comparable with that of the current study in which RMSE values of 4.03 TECu, 4.46 TECu and 10.06 TECu were obtained for DNN model driven with $F_{10.7}$, DNN model driven with EUV and NeQuick respectively within the solar cycle 2023.

Similar study was focussed on ionospheric TEC forecasting model based on deep learning, which consists of a CNN, LSTM neural network and Attention mechanism i.e. CNN-LSTM-Attention neural network mode [15]. Data used for the study were from 24 GNSS stations from the Crustal Movement Observation Network of China (CMONOC) and the model was driven with six parameters namely TEC time series, Bz, Kp, Dst, $F_{10.7}$ and hour of day. The model's performance was compared with NeQuick and LSTM, and CNN-LSTM. Results obtained showed RMSE values of 1.87 TECU, 3.59 TECu, 2.25 TECu and 2.07 TECU for the CNN-LSTM-Attention, NeQuick, LSTM, and CNN-LSTM respectively. The performance of the current study is a little lower than that of Ref. [15]. A study was done over the Brazilian region which was on feedforward artificial neural network based on a multilayer perceptron (MLP) approach for the prediction of TEC [21]. The configuration of the MLP used in their study is similar to that of the current study – both have 4 hidden layers though with different number of neurons in each layer. The prediction of their model was based on data collected on the previous 5 days. The accuracy of the model was evaluated by comparing the model predictions with real data and global ionosphere maps and the NeQuick G model. The TEC predictions were applied in single point positioning and errors obtained were 27% and 33% lower when compared to that of NeQuick G and global ionosphere maps, respectively.

Another study was based on CNN–GRU (CNN-Gate Recurrent Unit) neural network model to forecast the TEC during high solar activities from a single GNSS receiver at Sanya in Hainan, China [22]. Hourly vTEC values from September 2017 to August 2023 were used for training while nearly eight months of data from 2023 were used for testing. The performance of the CNN–GRU model obtained in their study was compared with the most used empirical models i.e. IRI and NeQuick models, and two artificial intelligence models i.e. GRU and SVM were also used for comparison. The results obtained showed RMSE values of 4.28 TECu, 4.51 TECU, 5.16 TECU, 9.38 TECU,12.11 TECU for CNN-GRU, GRU, SVM, IRI2020 and NeQuick2 respectively.

Parametric models like NeQuick 2 [3] and IRI [1] are models that are based on the parameters that represent the dynamics of a system being modeled. The ionosphere is dynamic and the factors that control or are responsible for its dynamics are time of the day, season of the year, level of solar activity and geomagnetic activities [23, 24]. Ionospheric models like the NeQuick 2 are built around these factors in order to forecast ionospheric parameters under different conditions.

Similar concepts have been used in training neural network (NN) for ionospheric predictions by using those factors as input parameters [12–17]. DNN is well-known to outperform ordinary NN [17]. In the current study, UT, DOY and $F_{10.7}$/EUV were used as input to represent time of the day, season of the year and level of solar activities respectively. Attempt was made in the current study to obtain the optimal hyperparameters (i.e. the number of hidden layers, neurons number in each hidden layer, batch number and epoch number) that define the network configuration for effective training and validation. Results obtained showed moderate error that is comparable to that of NeQuick 2 model during validation stage. This is consistent with previous studies on NN for ionospheric predictions [12, 16]. The study by Ref. [12] was on modeling M(3000)F2 and the results obtained were compared with IRI model - a standard ionospheric model like NeQuick 2. Their results showed that the trained NN model compared favourably with the IRI model.

In terms of the effectiveness of $F_{10.7}$ and EUV as solar ionizing indices, the results obtained showed that DNN driven with $F_{10.7}$ slightly performed better than the one driven by EUV. This

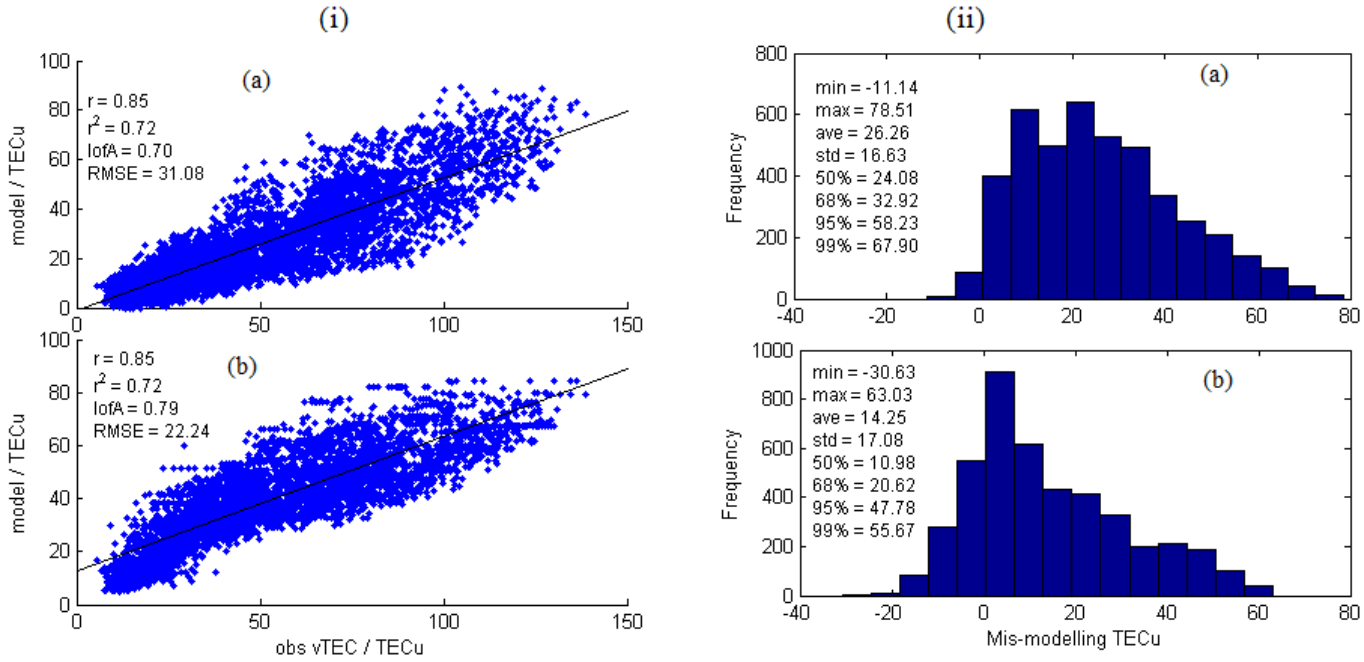

Figure 4: Diurnal plots of vTEC for the observed and models' predictions for 2000 as Figure 3. EUV values are not available for year 2000. Positive skewness is observed for the two models – which indicates underestimation of vTEC values.

result is consistent with that of Ref. [14] in which the effectiveness of sunspot number, $F_{10.7}$ and solar ultraviolet flux at 1 AU (Astronomical Unit) were tested for NN trainings. Their result showed that $F_{10.7}$ gave the least errors on the validation data set used. Validating the model outside of the solar cycle used for the training showed large deviation especially during solar maximum (i.e. year 2000) of solar cycle 23 – with solar maximum higher than that of the solar cycle 24 used for the training. This large deviation was not limited to DNN model alone – large deviation was also recorded for NeQuick 2 model. In the case of NeQuick 2 for year 2000, the underestimation might be due to $F_{10.7}$ saturation. By ITU (International Telecommunication Union) recommendation, and as stated in NeQuick 2 source code, maximum $F_{10.7}$ allowed as input into NeQuick 2 is 193 (or $R12 = 150$). This is to ensure that F2 layer critical frequency and M(3000)F2 from ITU-CCIR (Consultative Committee on International Radio) formulations are realistic [6]. Whereas for the DNN, $F_{10.7}$ of higher values like the ones in year 2000 were not used in the training – hence the possible reason for the large underestimation. Further research is required, especially for NeQuick 2 model during very high solar activity in order to further assess its performance and then propose possible modification to the existing $F_{10.7}$ cap limit.

4. Conclusion

DNN was configured and trained to model vTEC at a single station under a supervised learning condition using data for solar cycle 24. Unlike most of the previous studies which were based on predefined network models, deep learning NN was used in this study. A process of optimization was used to obtain the best configuration – which was done by varying the hyperparameters of the DNN model. The selected configuration has four hidden layers with neurons number of 32, 24, 16 and 8 in the hidden layers 1, 2, 3 and 4 respectively. EUV and $F_{10.7}$ were separately used as solar activity index in order to see which of these two indices will give a better result during training and validation. The performance of the DNN model was also compared with that of NeQuick 2 model. Observations in this study during validation showed that driving a DNN model with EUV and $F_{10.7}$ gave similar results in terms of performance i.e. deviation of predictions from the observed values. The validation of the two models (DNN and NeQuick 2 models) within the solar cycle 24 and for year 2021 outside the solar cycle 24 showed that the two models performed reasonably well. In general, there were good agreement between the models' predictions and the observed values, with DNN performing slightly better than NeQuick 2. However, large error was observed during a very high solar activity i.e. 2000 - a year of high solar maximum of the solar cycle 23. DNN and NeQuick 2 model largely underestimated vTEC – though NeQuick 2 performed better than DNN model in 2000. The observation during year 2000 might be due to the fact that the data set used for the training of the DNN were not of high solar activity as that of year 2000. Similarly, the $F_{10.7}$ cap value of 193 s.f.u could be the reason for the underestimation recorded in NeQuick 2 during year 2000. The study presented in this work could be extended to a global scale using similar approach.

Data availability

Solar index $F_{10.7}$ values are available at https://omniweb.gsfc.nasa.gov/form/dx1.html. EUV data are available from the TIMED SEE website at https://lasp.colorado.edu/lisird/data/timed_see_ssi_l3/. TEC values were retrieved from Ionex daily files obtained through the online archives of the Crustal Dynamics Data Information System (CDDIS), NASA Goddard Space Flight Center, Greenbelt, MD, USA. https://cddis.nasa.gov/archive/gnss/products/ionex/

Acknowledgment

The authors appreciate the Authority of the University of Ilorin for the continuous research support for the University of Ilorin Ionospheric and Space Research Group. O. A. Oladipo would like to appreciate ICTP associate scheme for awarding him regular associate for the period of 2018–2024 – the study presented in the paper was done during the period of the associateship.

References

[1] D. Bilitza, "International reference ionosphere 2000", Radio Science **36** (2000) 261. https://doi.org/10.1029/2000RS002432.

[2] G. Hochegger, B. Nava, S. M. Radicella & R. Leitinger, "A family of ionospheric models for different uses. Physics and chemistry of the earth, part C", Solar, Terrestrial & Planetary Science **25** (2000) 307. https://doi.org/10.1016/S1464-1917(00)00022-2.

[3] S. M. Radicella & R. Leitinger, "The evolution of the DGR approach to model electron density profiles", Advances in Space Research **27** (2001) 35. https://doi.org/10.1016/S0273-1177(00)00138-1.

[4] D. Bilitza & B. W. Reinisch, "International reference ionosphere 2007: Improvements and new parameters", Advances in Space Research **42** (2008) 599. https://doi.org/10.1016/j.asr.2007.07.048.

[5] S. M. Radicella & M. L. Zhang, "The improved DGR analytical model of electron density height profile and total electron content in the ionosphere", Annals of Geophysics **38** (1995) 35. https://doi.org/10.4401/ag-4130.

[6] R. Leitinger, M. L. Zhang & S. M. Radicella, "An improved bottomside for the ionospheric electron density model NeQuick", Annales Geophysicae **48** (2005) 525. https://doi.org/10.4401/ag-3217.

[7] B. Nava, P. Coïsson & S. M. Radicella, "A new version of the NeQuick ionosphere electron density model", Journal of Atmospheric and Solar-Terrestrial Physics **70** (2008) 1856. https://doi.org/10.1016/j.jastp.2008.01.015.

[8] J. N. Yao, B. Nava, O. K. Obrou & S. M. Radicella, "Validation of NeQuick2 model over West African equatorial region using GNSS-derived total electron content data", Journal of Atmospheric and Solar-Terrestrial Physics **181** (2018) 1. https://doi.org/10.1016/j.jastp.2018.10.001.

[9] A. Kashcheyev & B. Nava, "Validation of NeQuick 2 model topside ionosphere and plasmasphere electron content using COSMIC POD TEC", Journal of Geophysical Research: Space Physics **124** (2019). https://doi.org/10.1029/2019JA026971.

[10] D. Bilitza, M. Pezzopane, V. Truhlik, D. Altadill, B. W. Reinisch & A. Pignalberi, "The international reference ionosphere model: A review and description of an ionospheric benchmark", Reviews of Geophysics **60** (2022) e2022RG000792. https://doi.org/10.1029/2022RG000792.

[11] E. O. Oyeyemi, L. A. McKinnell & A. W. V. Poole, "Near-real time foF2 predictions using neural networks", Journal of Atmospheric and Solar-Terrestrial Physics **68** (2006) 1807. https://doi.org/10.1016/j.jastp.2006.07.002.

[12] E. O. Oyeyemi, L. A. McKinnell & A. M. V. Poole, "Neural network-based prediction techniques for global modeling of M(3000)F2 ionospheric parameter", Advances in Space Research **39** (2007) 643. https://doi.org/10.1016/j.asr.2006.09.038.

[13] D. Okoh, O. Owolabi, C. Ekechukwu, O. Folarin, G. Arhiwo, J. Agboe, S. Bolaji & B. Rabiu, "A regional GNSS-VTEC model over Nigeria using neural networks: A novel approach", Geodesy and Geodynamics **7** (2016) 19. https://doi.org/10.1016/j.geog.2016.03.003.

[14] D. Okoh, G. K. Seemala, B. Rabiu, J. B. Habarulema, S. Jin, K. Shiokawa, Y. Otsuka, M. Aggarwal, J. Uwamahoro, P. Mungufeni, S. Bolaji, A. A. Obafaye, N. Ellahony, C. H. Okonkwo, M. Tshisaphungo & D. J. Shetti, "A neural network-based ionospheric model over Africa from constellation observing system for meteorology, ionosphere, and climate and ground global positioning system observations", Journal of Geophysical Research: Space Physics **124** (2019). https://doi.org/10.1029/2019JA027065.

[15] J. Tang, Y. Li, M. Ding, H. Liu, D. Yang & X. Wu, "An ionospheric TEC forecasting model based on a CNN-LSTM-Attention mechanism neural network", Remote Sensing **14** (2022) 2433. https://doi.org/10.3390/rs14102433.

[16] O. M. Sorkhabi, "Deep learning of total electron content", SN Applied Sciences **3** (2021) 685. https://doi.org/10.1007/s42452-021-04674-6.

[17] A. V. Zhukov, Y. V. Yasyukevich & A. E. Bykov, "GIMLi: Global ionospheric total electron content model based on machine learning", GPS Solutions **25** (2021) 19. https://doi.org/10.1007/s10291-020-01055-1.

[18] M. Rothacher, G. Beutler, E. Brockmann, L. Mervart, S. Schaer, T. A. Springer, U. Wild, A. Wiget, C. Boucher & H. Seeger, "Annual report 1995 of the CODE analysis center of the IGS, astronomical institute", University of Berne (1995).

[19] C. J. Willmott, "On the validation of models", Phys. Geogr. **2** (1981) 184.

[20] G. B. Alemu & Y. G. Ejigu, "Prediction of ionospheric total electron content over low latitude region: Case study in Ethiopia", Adv. Space Res. **74** (2024) 284. https://doi.org/10.1016/j.asr.2024.03.062.

[21] A. Silva, A. Moraes, J. Sousasantos, M. Maximo, B. Vani & C. Faria Jr., "Using deep learning to map ionospheric total electron content over Brazil", Remote Sens. **15** (2023) 412. https://doi.org/10.3390/rs15020412.

[22] T. Y. Yang, J. Y. Lu, Y. Y. Yang, et al., "GNSS–VTEC prediction based on CNN–GRU neural network model during high solar activities", Sci. Rep. **15** (2025) 9109. https://doi.org/10.1038/s41598-025-93628-8.

[23] J. O. Adeniyi, O. A. Oladipo & S. M. Radicella, "Variability of foF2 and comparison with IRI map for an equatorial station", Journal of Atmospheric and Solar-Terrestrial Physics **69** (2007) 721. https://doi.org/10.1016/j.jastp.2006.12.001.

[24] O. A. Oladipo, J. O. Adeniyi, S. M. Radicella & O. B. Obrou, "Variability of equatorial ionospheric electron density at fixed heights below the F2 peak", Journal of Atmospheric and Solar-Terrestrial Physics **70** (2008) 1056. https://doi.org/10.1016/j.jastp.2008.01.004.